

Active Inverse Learning in Stackelberg Trajectory Games

William Ward, Yue Yu, Jacob Levy, Negar Mehr, David Fridovich-Keil, and Ufuk Topcu

Abstract—Game-theoretic inverse learning is the problem of inferring a player’s objectives from their actions. We formulate an inverse learning problem in a Stackelberg game between a leader and a follower, where each player’s action is the trajectory of a dynamical system. We propose an active inverse learning method for the leader to infer which hypothesis among a finite set of candidates best describes the follower’s objective function. Instead of using passively observed trajectories like existing methods, we actively maximize the differences in the follower’s trajectories under different hypotheses by optimizing the leader’s control inputs. Compared with uniformly random inputs, the optimized inputs accelerate the convergence of the estimated probability of different hypotheses conditioned on the follower’s trajectory. We demonstrate the proposed method in a receding-horizon repeated trajectory game and simulate the results using virtual TurtleBots in Gazebo.

I. INTRODUCTION

Learning to predict human behavior is a critical challenge in human-robot interaction. It enables robots to customize their strategies in various applications, including assisted driving [1], [2], traffic management [3], [4], and, in general, mitigating conflicts in human-in-the-loop robotic systems.

Game-theoretic inverse learning helps robots explain and predict human behavior in noncooperative interactions where humans actively optimize only their own objectives [5], [6], [7], [8], [9], [10], [11], [3]. The idea is to first model humans’ objectives as parameterized functions, then infer the parameter value such that the corresponding game-theoretic strategies—such as Nash or Stackelberg equilibrium strategies—match the humans’ actions in a dataset. Game-theoretic inverse learning is a necessary step in understanding human-robot interactions [12], [13], [3] and designing incentives for multiagent systems [14], [15].

The existing game-theoretic inverse learning methods are *passive*. In particular, these methods record the dataset of human actions before and independently of the inference process. Hence, some actions in the recorded dataset are uninformative for inference purposes, or simply redundant. As a result, in some settings, passive inverse learning is insufficient for rapid inferencing and online real-time decision-making [4].

In contrast to passive inverse learning, active inverse learning helps robots infer human intentions in cooperative inter-

actions by actively provoking informative human responses. For example, when learning objectives that explain a human’s ranking or rating of presented options, active inverse learning methods first provoke informative human responses and record them in the dataset, then infer the human’s objective function, and repeat this process if necessary [16], [17], [18], [19], [20]. These methods ensure that the human’s actions are informative by maximizing the volume removed from the hypothesis space [18], [21], [22], [23], [24], [25] or by maximizing the information gain [26], [27], [4], [28], [29], [30]. By integrating dataset updates with inference, active inverse learning provides practical solutions for inferring human intentions from limited interactions.

Despite its successes, active inverse learning still requires investigation in noncooperative interactions. The existing active inverse learning methods rely on querying humans who volunteer informative responses. In contrast, humans in noncooperative interactions only take actions that optimize their own objectives, regardless of whether or not the actions are informative. Therefore, how to provoke informative actions from noncooperative humans that reveal their objectives is, to our best knowledge, still an open question.

We study Stackelberg games, a specific class of noncooperative interactions between two players: a leader and a follower. In a Stackelberg game, the leader chooses an action, and then the follower responds by observing the leader’s behavior and optimizing its objective function.

We formulate an inverse learning problem in a Stackelberg game where a rational leader, such as a robot, infers which hypothesis among finitely many candidates best explains the behavior of a boundedly rational follower, such as a human. This problem is particularly relevant in shared autonomy, *e.g.*, when an autopilot must infer the type of a newly encountered human driver.

We model each player’s action as the trajectory of a linear time-invariant system. The follower tracks a linear function of the leader’s trajectory using a maximum-entropy linear quadratic regulator. The regulator contains a parameterized objective function and models bounded rationality in human decision-making [3]. The leader determines which hypothesis is most likely using the probability of each hypothesis conditioned on the follower’s state trajectory.

We propose an active inverse learning method to provoke informative trajectories from the follower by optimizing the leader’s inputs. In this optimization, we maximize the differences in the follower’s trajectory distributions under different hypotheses. We show that this optimization is a difference-of-convex program [31], which can be solved efficiently via the convex-concave procedure [32]. We evaluate

W. Ward, J. Levy, D. Fridovich-Keil, and U. Topcu are with the Oden Institute for Computational Engineering and Sciences at the University of Texas at Austin, Austin, TX, 78712, USA (emails: wward@utexas.edu, jake.levy@utexas.edu, dfk@utexas.edu, utopcu@utexas.edu). Y. Yu is with the Department of Aerospace Engineering and Mechanics at the University of Minnesota Twin Cities, Minneapolis, MN 55455 (email: yuey@umn.edu). N. Mehr is with the Department of Mechanical Engineering at the University of California Berkeley, Berkeley, CA, 94720, USA (email: negar@berkeley.edu).

the performance of the proposed method in a receding-horizon repeated trajectory game. Compared with random inputs, the leader inputs provided by our method accelerate the convergence of the probability of different hypotheses conditioned on the follower's trajectory.

Notation: We let \mathbb{R} , $\mathbb{R}_{\geq 0}$, and \mathbb{N} denote the set of real numbers, nonnegative real numbers, and nonnegative integers, respectively. We let $\mathbb{S}_{\geq 0}^n$ and $\mathbb{S}_{> 0}^n$ denote the set of n by n symmetric positive semidefinite and positive definite matrices, respectively. For any $x \in \mathbb{R}^n$, we let $\|x\| := \sqrt{x^\top x}$, $\|x\|_1 := \sum_{i=1}^n |x_i|$, $\|x\|_\infty := \max_{1 \leq i \leq n} |x_i|$, and $\|x\|_A^2 := x^\top A x$ for all $A \in \mathbb{S}_{> 0}^n$. We let 0_n denote the n -dimensional zero vector; I_n and $0_{n \times n}$ denote the n by n identity and zero matrix, respectively. We let $\mathcal{N}(\mu, \Sigma)$ denote the Gaussian distribution with mean $\mu \in \mathbb{R}^n$ and variance $\Sigma \in \mathbb{S}_{> 0}^n$. Given $n_1, n_2 \in \mathbb{N}$, we let $[n_1, n_2]$ denote the set of integers between n_1 and n_2 . Given $a_i \in \mathbb{R}^n$ for all $i \in \mathbb{N}$, we let $a_{i:j} := [a_i^\top \ a_{i+1}^\top \ \cdots \ a_j^\top]^\top$ for all $i < j$, $i, j \in \mathbb{N}$.

II. LINEAR QUADRATIC STACKELBERG TRAJECTORY GAMES

We introduce a Stackelberg game between a rational leader, such as a robot, and a boundedly rational follower, such as a human with noisy behavior. The players' actions are trajectories of stochastic linear time-invariant systems.

A. The dynamics of the players' systems

We assume that the leader's state evolves according to the following discrete-time linear time-invariant dynamics:

$$x_{t+1}^L = A^L x_t^L + B^L u_t^L + w_t^L \quad (1)$$

for all $t \in \mathbb{N}$, where $x_t^L \in \mathbb{R}^{n_L}$, $u_t^L \in \mathbb{R}^{m_L}$, and $w_t^L \in \mathbb{R}^{n_L}$ are the state, input, and disturbance of the system at time $t \in \mathbb{N}$, respectively; $A^L \in \mathbb{R}^{n_L \times n_L}$ and $B^L \in \mathbb{R}^{n_L \times m_L}$ are the leader's system parameters. In our experiments, Equation (1) to approximates the dynamics of a ground robot.

Similarly, the follower's state evolves according to the following dynamics:

$$x_{t+1}^F = A^F x_t^F + B^F u_t^F + w_t^F \quad (2)$$

for all $t \in \mathbb{N}$, where $x_t^F \in \mathbb{R}^{n_F}$, $u_t^F \in \mathbb{R}^{m_F}$, and $w_t^F \in \mathbb{R}^{n_F}$ denote the state, input, and disturbance of the system at time $t \in \mathbb{N}$, respectively; $A^F \in \mathbb{R}^{n_F \times n_F}$ and $B^F \in \mathbb{R}^{n_F \times m_F}$ are the follower's system parameters.

Throughout, we assume that the disturbances in the leader's system are independent, identically distributed Gaussian vectors. Similarly, the disturbances in the follower's system are independent, identically distributed Gaussian vectors. In other words, there exists $\Omega^L \in \mathbb{S}_{> 0}^{n_L}$ and $\Omega^F \in \mathbb{S}_{> 0}^{n_F}$ such that, for any $t \in \mathbb{N}$, we have

$$w_t^L \sim \mathcal{N}(0_{n_L}, \Omega^L), \quad w_t^F \sim \mathcal{N}(0_{n_F}, \Omega^F). \quad (3)$$

B. The players' objectives

We assume that the follower's objective is to track a linear function of the leader's trajectory. In particular, we let $M^F \in \mathbb{R}^{n_F \times n_L}$ denote the parameters of a linear transformation that maps the leader's internal state to an output reference observable to the follower. Let $x_{0:\tau}^L$ denote a leader trajectory of length $\tau \in \mathbb{N}$. The follower's objective is to simultaneously track the corresponding output trajectory $\{M^F x_0^L, M^F x_1^L, \dots, M^F x_\tau^L\}$ and minimize its input efforts.

We assume that the follower is boundedly rational and chooses its input according to the maximum entropy principle. Consequently, the distribution of u_t^F conditioned on x_t^F is Gaussian, i.e., $\mu_t^F | x_t^F \sim \mathcal{N}(\mu_t, \Sigma_t)$ for some $\mu_t \in \mathbb{R}^{m_F}$ and $\Sigma_t \in \mathbb{R}^{m_F \times m_F}$ [3]. In particular, $(\mu_{0:\tau-1}, \Sigma_{0:\tau-1})$ is optimal for the following stochastic trajectory optimization problem:

$$\begin{aligned} & \underset{\mu_{0:\tau-1}, \Sigma_{0:\tau-1}}{\text{minimize}} && \sum_{t=0}^{\tau} \mathbb{E} \left[\frac{1}{2} \|x_t^F - M^F x_t^L\|_{Q^F}^2 \right] \\ & && + \frac{1}{2} \sum_{t=0}^{\tau-1} \left(\mathbb{E} \left[\|u_t^F\|_{R^F}^2 \right] - \log \det \Sigma_t \right) \\ & \text{subject to} && x_{t+1}^F = A^F x_t^F + B^F u_t^F + w_t^F, \quad x_0^F = \hat{x}_0^F, \\ & && u_t^F | x_t^F \sim \mathcal{N}(\mu_t, \Sigma_t), \quad w_t^F \sim \mathcal{N}(0_{n_F}, \Omega^F), \\ & && t \in [0, \tau-1], \end{aligned} \quad (4)$$

where $\hat{x}_0^{n_F} \in \mathbb{R}^{n_F}$ is the initial state of the follower's system, $\mathbb{E}[\cdot]$ denotes the expectation; $Q^F \in \mathbb{S}_{> 0}^{n_F}$, and $R^F \in \mathbb{S}_{> 0}^{m_F}$ are the follower's cost parameters. The objective function in optimization (4) captures boundedly rational human decisions: it is noisy but centers around a cost-minimizing rational decision [33], [34], [35], [36], [37].

The following proposition provides a closed-form expression for the solution of optimization (4).

Proposition 1. *Let*

$$P_\tau^F = Q^F, \quad P_t^F = Q^F + (A^F)^\top P_{t+1}^F E_t^F, \quad (5a)$$

$$F_t^F = B^F (R^F + (B^F)^\top P_{t+1}^F B^F)^{-1} (B^F)^\top, \quad (5b)$$

$$E_t^F = A^F - F_t^F P_{t+1}^F A^F, \quad (5c)$$

$$q_\tau^F = -Q^F M^F x_\tau^L, \quad (5d)$$

$$q_t^F = (E_t^F)^\top q_{t+1}^F - Q^F M^F x_t^L, \quad (5e)$$

for all $t \in [0, \tau-1]$. Given $x_{0:\tau}^L$, $(\mu_{0:\tau-1}, \Sigma_{0:\tau-1})$ is optimal for optimization (4) if and only if

$$\Sigma_t = (R^F + (B^F)^\top P_{t+1}^F B^F)^{-1}, \quad (6a)$$

$$\mu_t = -\Sigma_t (B^F)^\top (P_{t+1}^F A^F x_t^F + q_{t+1}^F). \quad (6b)$$

for all $t \in [0, \tau-1]$. Furthermore, if the constraints in (4) hold, then $x_t^F \sim \mathcal{N}(\xi_t, \Lambda_t)$ for all $t \in [0, \tau]$, where

$$\xi_{t+1} = E_t^F \xi_t - F_t^F q_{t+1}^F, \quad (7a)$$

$$\Lambda_{t+1} = E_t^F \Lambda_t (E_t^F)^\top + F_t^F + \Omega^F, \quad (7b)$$

for all $t \in [0, \tau-1]$, with $\xi_0 = \hat{x}_0^F$ and $\Lambda_0 = 0_{n_F \times n_F}$.

Proof. See Appendix. \square

The leader's objective is to minimize a cost function that jointly depends on the follower's expected trajectory and the leader's trajectory. To this end, we assume that the leader

acts rationally and chooses its trajectory $x_{0:\tau}^L$ as a solution to the following trajectory optimization problem:

$$\begin{aligned} & \underset{u_{0:\tau-1}^L}{\text{minimize}} && \mathbb{E}[f(x_{0:\tau}^L, x_{0:\tau}^F)] + g(u_{0:\tau}^L) \\ & \text{subject to} && x_{t+1}^L = A^L x_t^L + B^L u_t^L + w_t^L, x_0^L = \hat{x}_0^L, \\ & && x_{t+1}^F = A^F x_t^F + B^F u_t^F + w_t^F, x_0^F = \hat{x}_0^F, \\ & && w_t^L \sim \mathcal{N}(0_{n_L}, \Omega^L), w_t^F \sim \mathcal{N}(0_{n_F}, \Omega^F), \\ & && u_t \in \mathbb{U}, u_t^F | x_t^F \sim \mathcal{N}(\mu_t, \Sigma_t), t \in [0, \tau-1], \\ & && (\mu_{0:\tau-1}, \Sigma_{0:\tau-1}) \text{ is optimal for (4),} \end{aligned} \quad (8)$$

where $\hat{x}_0^L \in \mathbb{R}^{n_L}$ is the initial state of the leader's system and $\mathbb{U} \subset \mathbb{R}^{m_F}$ is the set of feasible leader inputs at each time. Furthermore, $f : \mathbb{R}^{(n_L+1)n_L} \times \mathbb{R}^{(n_F+1)n_F} \rightarrow \mathbb{R}$ is the leader's cost function that jointly depends on the leader's state trajectory $x_{0:\tau}^L$ and the follower's state trajectory $x_{0:\tau}^F$; $g : \mathbb{R}^{\tau m_L} \rightarrow \mathbb{R}$ is a cost function that only depends on the leader's input trajectory. By choosing different functions for f and g , optimization (8) achieves different trade-offs between optimizing the leader and the follower's trajectory.

Problem (8) is a Stackelberg game, also known as a *bilevel optimization* problem. See [38] and references therein for a detailed discussion of bilevel optimization.

III. ACTIVE INVERSE LEARNING VIA DIFFERENCE MAXIMIZATION

Given the Stackelberg trajectory game introduced in Section II, we now consider the case where the leader does not know the parameter tuple (Q^F, R^F, M^F) in the follower's objective, except that it is one of finitely many candidates. In other words, the leader knows that there exist $Q^1, \dots, Q^d \in \mathbb{R}^{n_F \times n_F}$, $R^1, \dots, R^d \in \mathbb{R}^{m_F \times m_F}$, and $M^1, \dots, M^d \in \mathbb{R}^{n_F \times n_L}$ such that

$$(Q^F, R^F, M^F) = (Q^i, R^i, M^i) \quad (9)$$

for some $i \in [1, d]$. This case arises, for example, when a robot has already learned different types of human behavior offline but needs to determine the type of a newly encountered human via online interaction. In the following, we let $\theta^F := (Q^F, R^F, M^F)$ and $\theta^i := (Q^i, R^i, M^i)$ for all $i \in [1, d]$. We say that *hypothesis i is true* if (9) holds.

Based on a prior probability distribution of all hypotheses that gives the value of $\mathbb{P}(\theta^F = \theta^i | x_0^F)$ for all $i \in [1, d]$ and the follower's trajectory $x_{1:\tau}^F$, the leader can infer whether hypothesis i is more likely to be true than hypothesis j by computing the following ratio:

$$\frac{\mathbb{P}(\theta^F = \theta^i | x_{0:\tau}^F)}{\mathbb{P}(\theta^F = \theta^j | x_{0:\tau}^F)} = \frac{\mathbb{P}(\theta^F = \theta^i | x_0^F) \mathbb{P}(x_{1:\tau}^F | \theta^F = \theta^i)}{\mathbb{P}(\theta^F = \theta^j | x_0^F) \mathbb{P}(x_{1:\tau}^F | \theta^F = \theta^j)}. \quad (10)$$

If the ratio in (10) is greater than one, then trajectory $x_{0:\tau}^F$ is more likely to occur under hypothesis i than under hypothesis j , and vice versa.

However, observing the follower's trajectory can be uninformative for the inference above if the trajectories under different hypotheses are similar. For example, suppose that

$$\mathbb{P}(x_{1:\tau}^F | \theta^F = \theta^i) \approx \mathbb{P}(x_{1:\tau}^F | \theta^F = \theta^j) \quad (11)$$

for some $i \neq j$; then, (10) implies that $\frac{\mathbb{P}(\theta^F = \theta^i | x_{0:\tau}^F)}{\mathbb{P}(\theta^F = \theta^j | x_{0:\tau}^F)} \approx \frac{\mathbb{P}(\theta^F = \theta^i | x_0^F)}{\mathbb{P}(\theta^F = \theta^j | x_0^F)}$. In other words, observing the follower's ongoing trajectory $x_{1:\tau}^F$ does not help the leader distinguish hypothesis i from j . In the following, we discuss how the leader can actively avoid the scenarios where (11) happens.

A. The follower's trajectories under different hypotheses

To avoid the scenarios where (11) happens, it suffices to make the follower's trajectory distributions under different hypotheses as different as possible. To this end, we first take a closer look at the follower's trajectory. Proposition 1 shows that the follower's state at each time is a Gaussian random variable. Particularly, let

$$E_t^i = A^F - F_t^i P_{t+1}^i A^F, \quad (12a)$$

$$F_t^i = B^F (R^i + (B^F)^\top P_{t+1}^i B^F)^{-1} (B^F)^\top, \quad (12b)$$

$$P_\tau^i = Q^i, P_t^i = Q^i + (A^F)^\top P_{t+1}^i E_t^i, \quad (12c)$$

$$\Lambda_0^i = 0_{n_F \times n_F}, \Lambda_{t+1}^i = E_t^i \Lambda_t^i (E_t^i)^\top + F_t^i + \Omega^F, \quad (12d)$$

$$q_\tau^i = -Q^i M^i x_\tau^L, \quad (12e)$$

$$q_t^i = (E_t^i)^\top q_{t+1}^i - Q^i M^i x_t^L, \quad (12f)$$

$$\xi_0^i = \hat{x}_0^F, \xi_{t+1}^i = E_t^i \xi_t^i + F_t^i q_{t+1}^i, \quad (12g)$$

for all $t \in [0, \tau-1]$. Proposition 1 implies that, if hypothesis i is true, i.e., $\theta^F = \theta^i$, then

$$x_t^F \sim \mathcal{G}_t^i := \mathcal{N}(\xi_t^i, \Lambda_t^i). \quad (13)$$

To measure the differences between the trajectory distribution under different hypotheses, we introduce a distance function. To this end, let

$$\mathbb{D} := \{(i, j) \mid i < j, i, j \in [1, d]\}. \quad (14)$$

We propose the following function

$$D(\mathcal{G}_t^i, \mathcal{G}_t^j) := \left\| \xi_t^i - \xi_t^j \right\|_{(\Lambda_t^i)^{-1} + (\Lambda_t^j)^{-1}}^2 \quad (15)$$

for all $t \in [1, \tau]$ and $(i, j) \in \mathbb{D}$. Notice that, since $\Omega^F \in \mathbb{S}_{>0}^{n_F}$, (12) implies that $\Lambda_t^i \in \mathbb{S}_{>0}^{n_F}$ for all $t \in [1, \tau]$ and $k \in [1, d]$. One can verify that the distance function in (15) is proportional to the sum of the KL-divergence from \mathcal{G}_t^i to \mathcal{G}_t^j and the KL-divergence from \mathcal{G}_t^j to \mathcal{G}_t^i , up to some additive constants. Later, we use this function to optimize the leader's inputs.

The intuition behind this distance function is to first evaluate (up to a constant of 2, for the convenience of notation) the sum of $D_{KL}(\mathcal{G}_t^i || \mathcal{G}_t^j)$ and $D_{KL}(\mathcal{G}_t^j || \mathcal{G}_t^i)$, then remove the terms that are independent of ξ_t^i and ξ_t^j , which are, as suggested by (12), independent of the leader's trajectory.

B. Maximizing the worst-case pairwise distance

To avoid the scenarios where (11) happens, we need to maximize the value of the distance function in (15) for any $(i, j) \in \mathbb{D}$. To this end, we define the following *worst-case*

distance function, which evaluates the minimum value of function (15) among all $(i, j) \in \mathbb{D}$:

$$\begin{aligned} & \min_{(i,j) \in \mathbb{D}} \left\{ \sum_{t=1}^{\tau} \left\| \xi_t^i - \xi_t^j \right\|_{(\Lambda_t^i)^{-1} + (\Lambda_t^j)^{-1}}^2 \right\} \\ &= \sum_{(i,j) \in \mathbb{D}} \sum_{t=1}^{\tau} \left\| \xi_t^i - \xi_t^j \right\|_{(\Lambda_t^i)^{-1} + (\Lambda_t^j)^{-1}}^2 \\ & - \max_{(i,j) \in \mathbb{D}} \left\{ \sum_{(k,l) \in \mathbb{D} \setminus \{(i,j)\}} \sum_{t=1}^{\tau} \left\| \xi_t^k - \xi_t^l \right\|_{(\Lambda_t^k)^{-1} + (\Lambda_t^l)^{-1}}^2 \right\}. \end{aligned} \quad (16)$$

The second step in (16) uses the fact that, given any $\alpha_1, \dots, \alpha_n \in \mathbb{R}$, we have

$$\min_{i \in [1,n]} \alpha_i = \sum_{i \in [1,n]} \alpha_i - \max_{i \in [1,n]} \sum_{j \in [1,n], j \neq i} \alpha_j.$$

Notice that the distance in (16) does not include the terms for $t = 0$ because, due to (12), $\xi_0^i = \xi_0^j$ for all $(i, j) \in \mathbb{D}$.

Based on the worst-case distance in (16), we propose optimizing the leader's input trajectory $u_{0:\tau-1}^L$ by solving optimization (17) (see next page) instead of optimization (8). In (17), E_t^i, F_t^i and Λ_t^i are given by (12). Also, we approximate the leader's state trajectory $x_{0:\tau}^L$ with its expectation, denoted by $\eta_{0:\tau}$, which satisfies the averaged dynamics $\eta_{t+1} = A^L \eta_t + B^L u_t^L$. Notice that this approximation replaces the disturbance term w_t^L in (8) with its mean, given by $w_t^L = 0_{n_L}$ in (3).

Additionally, optimization (17) replaces $\mathbb{E}[f(x_{0:\tau}^L, x_{0:\tau}^F)]$ in (8) with the negative of the worst-case distance in (16). In particular, the constraints in (17) imply that

$$\max_{(i,j) \in \mathbb{D}} \left\{ \sum_{(k,l) \in \mathbb{D} \setminus \{(i,j)\}} \sum_{t=1}^{\tau} \left\| \xi_t^k - \xi_t^l \right\|_{(\Lambda_t^k)^{-1} + (\Lambda_t^l)^{-1}}^2 \right\} \leq s.$$

Since the objective function in (17) minimizes the value of s , the above inequality holds as an equality at optimality. Hence, the objective function in (17) is equivalent to the one in (8), except we replace $\mathbb{E}[f(x_{0:\tau}^L, x_{0:\tau}^F)]$ in (8) with the negative of the worst-case distance in (16). The idea of this replacement is to maximize the worst-case distance in (16), ensuring that the distance in (15) is large for any $(i, j) \in \mathbb{D}$. Thus, any pair of hypotheses are easily distinguished.

Optimization (17) is a difference-of-convex program: all of its constraints are convex, but its objective function is the difference between two convex functions [31]. A popular solution method for difference-of-convex programs is the *convex-concave procedure*, which guarantees global convergence to a stationary point [39] and provides locally optimal solutions in practice [32].

IV. NUMERICAL EXPERIMENTS AND SIMULATIONS

We empirically demonstrate our results using two receding-horizon repeated trajectory games between a boundedly rational follower and a rational leader. In the first game, a ground rover controlled by the follower pursues one of $d = 3$ rovers controlled by the leader. At each time step, the agents play a Stackelberg trajectory game and implement only the first step of their respective input trajectories. The leader infers which leading rover the follower is following. In

the second game, the leader (a driving assistant) recommends a trajectory for the follower's rover to track. The leader must infer the follower's driving type from $d = 3$ known possibilities (e.g., someone who drives fast, drives slow, or obeys the speed limit) based on how the follower responds to the leader's suggestion.

We solve the optimization problems for each game in Julia [40] using the JuMP [41] and MOSEK [42] tools. Then, we convert the optimized trajectories into splines and transmit them to simulated TurtleBots [43] in ROS/Gazebo via virtual communication ports [44], [45]. The TurtleBots follow the trajectory splines using proportional gain controllers that adjust their linear and angular velocity over time. Since the TurtleBots' speed and maneuverability are limited by their simulated dynamics in Gazebo, we tune the game parameters to ensure that the optimized trajectories are feasible, as described in the following subsections. Note that we run ROS Noetic on Ubuntu Jammy (22.04) using the RoboStack virtual environment [46].

A. Leader-follower pursuit game parameters

We define the parameters for the leader-follower pursuit game as follows. We model the follower's dynamics using an instance of (2), where $A^F = \exp\left(\delta \begin{bmatrix} 0_{2 \times 2} & I_2 \\ 0_{2 \times 2} & 0_{2 \times 2} \end{bmatrix}\right)$, $B^F = \int_0^\delta \exp\left(t \begin{bmatrix} 0_{2 \times 2} & I_2 \\ 0_{2 \times 2} & 0_{2 \times 2} \end{bmatrix}\right) dt \begin{bmatrix} 0_{2 \times 2} \\ I_2 \end{bmatrix}$, $\Omega^F = 1 \times 10^{-5} I_4$, and $\delta = 2$ seconds is the discretization step size. We model the leader's dynamics using the joint dynamics of $d \in \mathbb{N}$ double-integrators, where $A^L = I_d \otimes A^F$, $B^L = I_d \otimes B^F$, and $\Omega^L = 1 \times 10^{-5} I_{4d \times 4d}$. For the follower's trajectory optimization in (4), we let $Q^i = 20 \text{diag}([1 \ 1 \ 0 \ 0])$, $R^i = 3 \times 10^4 I_2$, and $M^i = [0_{4 \times 4(i-1)} \ I_4 \ 0_{4 \times 4(d-i)}]$ for all $i \in [1, d]$. For the leader's trajectory optimization in (8), we let $\mathbb{U} := \{u \in \mathbb{R}^{2d} \mid \|u\|_\infty \leq 5 \times 10^{-3}\}$, and $g(u_{0:\tau-1}^L) = \sum_{t=1}^{\tau-2} \|u_{t+1}^L - u_t^L\|^2$. Additionally, we constrain the velocity components of each leading rover's trajectory as follows to ensure dynamic feasibility in the simulation:

$$\left\| \begin{bmatrix} 0_{2 \times 2} & I_2 \\ 0_{2 \times 2} & I_2 \\ 0_{2 \times 2} & I_2 \end{bmatrix} x_t^L \right\|_\infty \leq 0.1 \text{m/s}.$$

B. Driving assistant game parameters

Similarly, in the driving assistant game, we model the follower's dynamics using an instance of (2), where $A^F = \exp\left(\delta \begin{bmatrix} 0_{2 \times 2} & I_2 \\ 0_{2 \times 2} & 0_{2 \times 2} \end{bmatrix}\right)$, $B^F = \int_0^\delta \exp\left(t \begin{bmatrix} 0_{2 \times 2} & I_2 \\ 0_{2 \times 2} & 0_{2 \times 2} \end{bmatrix}\right) dt \begin{bmatrix} 0_{2 \times 2} \\ I_2 \end{bmatrix}$, $\Omega^F = 1 \times 10^{-4} I_4$, and $\delta = 2$ seconds. We model the leader's dynamics using an instance of (1), where $A^L = A^F$, $B^L = B^F$, and $\Omega^L = 1 \times 10^{-7} I_4$. For the follower's trajectory optimization in (4), we let $Q^i = \text{diag}([1000 \ 100 \ 100 \ 100])$ and $R^i = \text{diag}([1 \times 10^4 \ 1000])$. Then, we model three follower driver types, each with a unique M^i . Given the leader's suggested trajectory, type 1 scales down the velocity ($M^1 = \text{diag}([0.95 \ 0.85 \ 0.95 \ 0.85])$), type 2 follows the suggested velocity ($M^2 = I_4$), and type 3 scales up the velocity ($M^3 = \text{diag}([1.05 \ 1.15 \ 1.05 \ 1.15])$).

$$\begin{aligned}
& \underset{s, u_{0:\tau-1}^L}{\text{minimize}} && s - \sum_{(i,j) \in \mathbb{D}} \sum_{t=0}^{\tau} \left\| \xi_t^i - \xi_t^j \right\|_{(\Lambda_i^i)^{-1} + (\Lambda_j^j)^{-1}}^2 + g(u_{0:\tau-1}) \\
& \text{subject to} && \eta_{t+1}^L = A^L \eta_t^L + B^L u_t^L, \eta_0^L = \hat{x}_0^L, \\
& && q_t^i = (E_t^i)^\top q_{t+1}^i - Q^i M^i \eta_t, q_\tau^i = -Q^i M^i \eta_\tau, \xi_{t+1}^i = E_t^i \xi_t^i - F_t^i q_{t+1}^i, \xi_0^i = \hat{x}_0^F, \\
& && \sum_{(k,l) \in \mathbb{D} \setminus \{(i,j)\}} \sum_{t=1}^{\tau} \left\| \xi_t^k - \xi_t^l \right\|_{(\Lambda^k)^{-1} + (\Lambda^l)^{-1}}^2 \leq s, \forall t \in [0, \tau-1], i \in [1, d], (i, j) \in \mathbb{D}.
\end{aligned} \tag{17}$$

For the leader's trajectory optimization in (8), we let $\mathbb{U} := \{u \in \mathbb{R}^{2d} \mid \|u\|_\infty \leq 5 \times 10^{-2}\}$, and $g(u_{0:\tau-1}^L) = \sum_{t=1}^{\tau-2} \|u_{t+1}^L - u_t^L\|^2$.

Additionally, we constrain the leader and follower trajectories within the boundaries of a sideways "L" shaped road. The road width $r_w = 1.3$ meters, and the road length of the short segment $r_l = 3$ meters. The follower should neither drive backwards nor drive off the road. Therefore, during the first road segment, for all $t \in [1, \frac{\tau}{2}]$, we apply the following constraints: $[0 \ 1 \ 0 \ 0]x_t^L \geq 0$ m, $[0 \ 0 \ 0 \ 1]x_t^L \geq 0$ m/s, and $\|[1 \ 0 \ 0 \ 0]x_t^F\|_\infty \leq 0.5r_w$. Similarly, during the second road segment, for all $t \in [\frac{\tau}{2}, \tau]$, $[1 \ 0 \ 0 \ 0]x_t^L \geq -0.5r_w$, $[0 \ 0 \ 1 \ 0]x_t^L \geq 0$ m/s, and $r_l \leq [0 \ 1 \ 0 \ 0]x_t^F \leq r_l + r_w$.

C. Experimental procedure

We demonstrate the proposed learning methods using the simulation of two receding-horizon repeated trajectory games. At time $t\delta$, for some $t \in \mathbb{N}$, the leader observes its current state \hat{x}_t^L and the follower's current state \hat{x}_t^F . Then, the leader solves optimization (17) with $\hat{x}_0^L = \hat{x}_t^L$ and $\hat{x}_0^F = \hat{x}_t^F$ to obtain the optimal input sequence $u_{0:\tau-1}^L$. Next, the leader simulates a state trajectory $x_{0:\tau-1}^L$ according to (1), shares the trajectory with the follower, and applies u_0^L to its system. Meanwhile, at time $t\delta$, the follower observes its current state \hat{x}_t^F and receives the leader's simulated trajectory $x_{0:\tau}^L$. The follower solves optimization (4) with $\hat{x}_0^F = \hat{x}_t^F$ and obtains the optimal mean and covariance sequences $(\mu_{0:\tau-1}, \Sigma_{0:\tau-1})$. Finally, the follower samples $u_0^F \sim \mathcal{N}(\mu_0, \Sigma_0)$ and applies u_0^F to its system.

D. Results

We simulate the players' trajectories by solving the leader's trajectory optimization (17) using the convex-concave procedure [32]. Fig. 1a shows the results of the leader-follower pursuit game. To maximize the differences between the follower's trajectories under different hypotheses, optimization (17) ensures that different leading rovers move in different directions. Fig. 1b shows the results of the driving assistant game. Optimization (17) ensures that the leader suggests a trajectory to the follower that clearly distinguishes the follower's response under each driver type.

We further showcase the advantage of the proposed method in terms of distinguishing different hypotheses. Let $p^* = [1 \ 0 \ \dots \ 0]^\top \in \mathbb{R}^d$ denote the ground truth probability of all hypotheses. Without loss of generality, we assume $(Q^F, R^F, M^F) = (Q^1, R^1, M^1)$. In addition, let p^t denote the d -dimensional vector such that

$$p_i^t := \mathbb{P}((Q^F, R^F, M^F) = (Q^i, R^i, M^i) \mid \bar{x}_{0:t}^F) \tag{18}$$

for all $i \in [1, d]$, where we let $\mathbb{P}((Q^F, R^F, M^F) = (Q^i, R^i, M^i) \mid \bar{x}_0^F) := \frac{1}{d}$ for all $i \in [1, d]$. That is, we choose the uniform distribution as the leader's prior distribution over all hypotheses given the follower's initial state. Notice that one can compute p^t recursively using Bayes rule.

Fig. 2 shows the time history of the ℓ_1 -norm distance between p^t and p^* and compares the results to where the leader uses randomly sampled trajectories. We generate the random trajectories in two steps. First, we sample a trajectory from a uniform distribution over a set of allowable states. Second, we solve an instance of optimization (4), where the leader follows the random trajectory as close as possible without violating its dynamics.

In the pursuit game, we constrain the random positions within ± 0.3 m and the velocities within ± 0.1 m/s. In the driving assistant game, we constrain the random positions within the road boundaries (defined in section IV-B). In the first road segment, we constrain the horizontal and vertical velocities, respectively, within ± 1.3 and $(0, 0.5)$ m/s. Similarly, in the second road segment, we constrain the velocities within $(0, 1.3)$ and ± 0.5 m/s.

The results in Fig. 2 show that p^t converges faster to p^* when the leader uses our proposed method, versus randomly generated trajectories. In the pursuit game, the proposed method consistently achieves orders of magnitude better convergence than the random trajectories. However, in the driving game, the proposed method only shows significant gains after the first six seconds. The driving game is a lower dimensional problem than the pursuit game, and the road boundaries add additional state constraints. As a result, it is more difficult to distinguish between the hypotheses.

We simulate the experiments in Gazebo (see Fig. 3). We provide a video of our Gazebo simulations at <https://youtu.be/csQpXJh1SmM> and our code at https://github.com/u-t-autonomous/active_inverse_stackelberg and https://github.com/willward20/active_inverse_stackelberg_ros.

V. CONCLUSION

We formulated an inverse learning problem in a Stackelberg trajectory game, where the leader infers the type of the follower's cost function by observing its trajectories. We proposed an active inverse learning method to accelerate the leader inference by making the follower's trajectories under different hypotheses as different as possible. This method provides faster convergence of the probability of different hypotheses when compared against random inputs.

However, the current work still has limitations. For example, it considers neither nonlinear dynamics nor collision avoidance in the players' trajectory optimization. In addition,

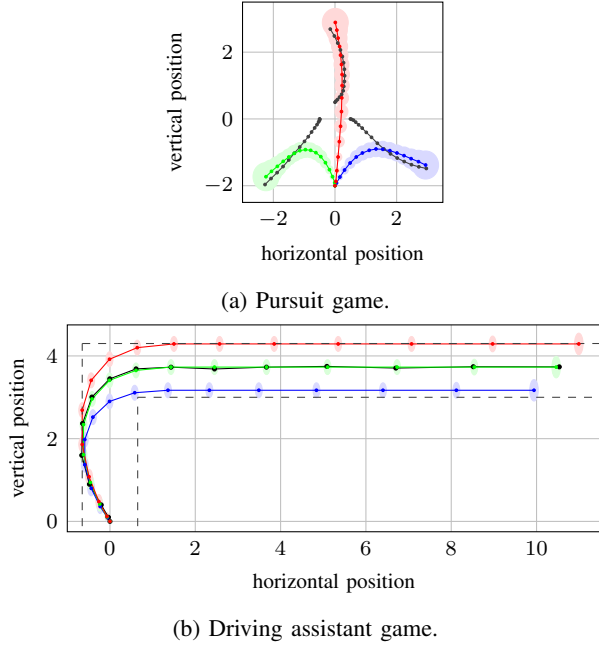


Fig. 1: The trajectories of the leader (black) and followers under different hypotheses. Each color indicates one of the hypotheses. The semi-axis of the shaded ellipses represents the directions of the eigenvectors of the corresponding covariance matrices.

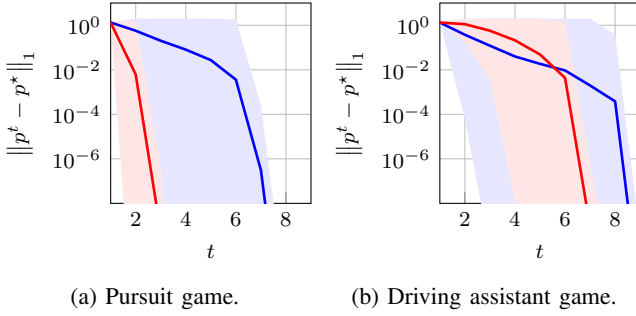


Fig. 2: Comparing the convergence of p^t when using the proposed method (red) versus sampling a random trajectory (blue). The solid lines show the median over 100 simulations, while the boundaries of the colored areas mark the corresponding first and third quartiles.

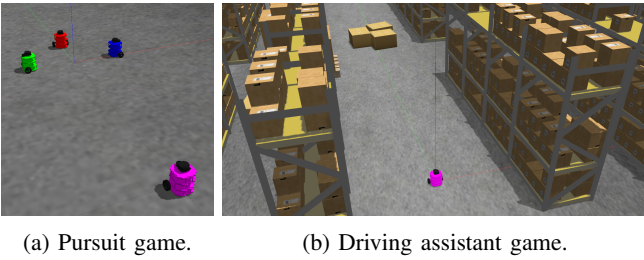


Fig. 3: Simulating the results on TurtleBots in a virtual warehouse environment in Gazebo.

it ignores the possibility of deceptive actions of the follower. In future work, we plan to address these limitations and develop information-gathering strategies in general Bayesian games.

APPENDIX

Proof of Proposition 1

Given $y \in \mathbb{R}^{n_F}$ and $t \in [0, \tau]$, let

$$\begin{aligned} \psi_t(y, \mu_{t:\tau}, \Sigma_{t:\tau}) \\ := \sum_{j=t}^{\tau} \mathbb{E} \left[\frac{1}{2} \|x_j^F - M^F x_j^L\|_{Q^F}^2 \mid x_t^F = y \right] \\ + \frac{1}{2} \sum_{j=t}^{\tau-1} \left(\mathbb{E} \left[\|u_j^F\|_{R^F}^2 \mid x_t^F = y \right] - \log \det \Sigma_j \right). \end{aligned} \quad (19)$$

where $x_{j+1}^F = A^F x_j^F + B^F u_j^F$ and $u_j^F \sim \mathcal{N}(\mu_j, \Sigma_j)$. Furthermore, let $V_t(y) := \min_{\mu_{t:\tau-1}, \Sigma_{t:\tau-1}} \psi_t(y, \mu_{t:\tau}, \Sigma_{t:\tau})$ for all $t \in [0, \tau]$. Then one can verify that the optimal value of optimization (4) is $V(\hat{x}_0^F)$. In addition, we can show that $V_\tau(y) = \frac{1}{2} y^\top Q^F y - \langle Q^F M^F x_\tau^L, y \rangle + \frac{1}{2} \|M^F x_\tau^L\|_{Q^F}^2$, i.e., $V_\tau(y)$ is a quadratic function of y . Suppose that $V_{t+1}(y)$ is a quadratic function of y , i.e., there exists $P_{t+1}^F \in \mathbb{R}^{n_F \times n_F}$, $q_{t+1}^F \in \mathbb{R}^{n_F}$, and $\nu_{t+1}^F \in \mathbb{R}$, such that $V_{t+1}(y) = \frac{1}{2} y^\top P_{t+1}^F y + \langle q_{t+1}^F, y \rangle + \nu_{t+1}^F$. Then the principle of dynamic programming together imply that

$$\begin{aligned} V_t(y) &= \frac{1}{2} \|y - M^F x_t^F\|_{Q^F}^2 - \frac{1}{2} \log \det \Sigma_t \\ &+ \min_{\mu_t, \Sigma_t} \mathbb{E} \left[\frac{1}{2} \|u_t^F\|_{R^F}^2 + V_{t+1}(A^F x_t^F + B^F u_t^F + w_t^F) \mid x_t^F = y \right], \end{aligned} \quad (20)$$

where $u_t^F \mid x_t^F \sim \mathcal{N}(\mu_t, \Sigma_t)$. Observe that

$$\begin{aligned} \mathbb{E}[\|u_t^F\|_{R^F}^2 \mid x_t^F = y] \\ = \mu_t^\top R^F \mu_t + \mathbb{E}[\text{tr}((u_t^F - \mu_t)(u_t^F - \mu_t)^\top R^F) \mid x_t^F = y] \\ = \mu_t^\top R^F \mu_t + \text{tr}(\Sigma_t R^F). \end{aligned} \quad (21)$$

In addition, we can show that

$$\begin{aligned} \mathbb{E}[V_{t+1}(A^F x_t^F + B^F u_t^F + w_t^F) \mid x_t^F = y] \\ = \frac{1}{2} (A^F y + B^F \mu_t)^\top P_{t+1}^F (A^F y + B^F \mu_t) \\ + \mathbb{E}[(A^F x_t^F + B^F \mu_t)^\top P_{t+1}^F B^F (u_t^F - \mu_t) \mid x_t^F = y] \\ + \frac{1}{2} \mathbb{E}[(B^F (u_t^F - \mu_t))^\top P_{t+1}^F B^F (u_t^F - \mu_t) \mid x_t^F = y] \\ + \langle q_{t+1}^F, A^F y + B^F \mu_t \rangle + \frac{1}{2} \mathbb{E}[\text{tr}(w_t^F (w_t^F)^\top P_{t+1}^F)] + \nu_{t+1}^F \\ = \frac{1}{2} (A^F y + B^F \mu_t)^\top P_{t+1}^F (A^F y + B^F \mu_t) + \frac{1}{2} \text{tr}(\Omega^F P_{t+1}^F) \\ + \frac{1}{2} \text{tr}(\Sigma_t (B^F)^\top P_{t+1}^F B^F) + \langle q_{t+1}^F, A^F y + B^F \mu_t \rangle + \nu_{t+1}^F. \end{aligned} \quad (22)$$

Substituting (22) and (21) into (20) gives

$$\begin{aligned} V_t(y) &= \frac{1}{2} \text{tr}(\Sigma_t R^F + \Omega^F P_{t+1}^F + (B^F)^\top P_{t+1}^F B^F) + \nu_{t+1}^F \\ &+ \frac{1}{2} y^\top (Q^F + (A^F)^\top P_{t+1}^F A^F) y + \langle A^\top q_{t+1}^F - Q^F M^F x_t^L, y \rangle \\ &+ \frac{1}{2} \mu_t^\top (R^F + (B^F)^\top P_{t+1}^F B^F) \mu_t + \frac{1}{2} (x_t^L)^\top (M^F)^\top Q^F M^F x_t^L \\ &+ \langle (B^F)^\top q_{t+1}^F + (B^F)^\top P_{t+1}^F A^F y, \mu_t \rangle - \frac{1}{2} \log \det \Sigma_t. \end{aligned} \quad (23)$$

By setting the derivative of $V_t(y)$ with respect to μ_t and Σ_t to zero, we obtain (6). By substituting (6) into (23), we can show that $V_t(y) = \frac{1}{2} y^\top P_t^F y + \langle q_t^F, y \rangle + \nu_t^F$, where Q_t^F and q_t^F satisfy (5).

Next, let $K_t = -\Sigma_t(B^F)^\top P_{t+1}^F A^F$ and $b_t = -\Sigma_t(B^F)^\top q_{t+1}^F$. Then (6) implies that $u_t^F | x_t^F \sim \mathcal{N}(K_t x_t^F + b_t, \Sigma_t)$. Since $x_0^F = \hat{x}_0^F$, by using the results in [47, p. 91] we can show the following:

$$\begin{bmatrix} x_1^F \\ u_1^F \end{bmatrix} \sim \mathcal{N} \left(\begin{bmatrix} \xi_0 \\ K_0 \xi_0 + b_0 \end{bmatrix}, \begin{bmatrix} \Lambda_0 & K_0 \Lambda_0 \\ \Lambda_0 K_0^\top & \Sigma_0 + K_0^\top \Lambda_0 K_0 \end{bmatrix} \right).$$

Therefore $x_{t+1}^F = A^F x_t^F + B^F u_t^F + w_t^F \sim \mathcal{N}(\xi_1, \Lambda_1)$, where ξ_1 and Σ_1 satisfy (7). By repeating similar steps for $t \in [2, \tau]$ we can show that (7) holds for all $t \in [0, \tau - 1]$, which completes the proof.

ACKNOWLEDGMENT

This work was supported by a National Science Foundation CAREER award under Grant No. 2336840, as well as the following NSF grants: ECCS-2145134, CNS-2218759, and CCF-2211542. Additionally, this work was supported by ONR subcontracts with Phillips (N00014-24-S-B001) and the University of Pennsylvania (N00014-20-1-2115).

REFERENCES

- [1] V. A. Shia, Y. Gao, R. Vasudevan, K. D. Campbell, T. Lin, F. Borrelli, and R. Bajcsy, "Semiautonomous vehicular control using driver modeling," *IEEE Trans. Intel. Transp. Syst.*, vol. 15, no. 6, pp. 2696–2709, 2014.
- [2] N. Mehr, R. Horowitz, and A. D. Dragan, "Inferring and assisting with constraints in shared autonomy," in *Proc. IEEE Conf. Decision Control*. IEEE, 2016, pp. 6689–6696.
- [3] N. Mehr, M. Wang, M. Bhatt, and M. Schwager, "Maximum-entropy multi-agent dynamic games: Forward and inverse solutions," *IEEE Trans. Robot.*, 2023.
- [4] D. Sadigh, S. S. Sastry, S. A. Seshia, and A. Dragan, "Information gathering actions over human internal state," in *Proc. Int. Conf. Intel. Robots Syst.*. IEEE, 2016, pp. 66–73.
- [5] K. Waugh, B. D. Ziebart, and J. A. Bagnell, "Inverse correlated equilibrium for matrix games," *Adv. Neural Inform. Process. Syst.*, 2010.
- [6] V. Kuleshov and O. Schrijvers, "Inverse game theory: Learning utilities in succinct games," in *Int. Conf. Web Internet Econ.*. Springer, 2015, pp. 413–427.
- [7] D. Bertsimas, V. Gupta, and I. C. Paschalidis, "Data-driven estimation in equilibrium using inverse optimization," *Math. Prog.*, vol. 153, no. 2, pp. 595–633, 2015.
- [8] L. Peters, D. Fridovich-Keil, V. R. Royo, C. J. Tomlin, and C. Stachniss, "Inferring objectives in continuous dynamic games from noise-corrupted partial state observations," in *Robotics: Sci. and Syst. 2021*, 2021.
- [9] T. L. Molloy, J. I. Charaja, S. Hohmann, and T. Perez, "Inverse optimal control and inverse noncooperative dynamic game theory," 2022.
- [10] Y. Yu, J. Salfity, D. Fridovich-Keil, and U. Topcu, "Inverse matrix games with unique quantal response equilibrium," *IEEE Control Syst. Lett.*, vol. 7, pp. 643–648, 2022.
- [11] J. Li, C.-Y. Chiu, L. Peters, S. Sojoudi, C. Tomlin, and D. Fridovich-Keil, "Cost inference for feedback dynamic games from noisy partial state observations and incomplete trajectories," in *Proc. Int. Conf. Auton. Agents and Multiagent Syst.*, 2023, pp. 1062–1070.
- [12] C. K. Ling, F. Fang, and J. Z. Kolter, "What game are we playing? end-to-end learning in normal and extensive form games," in *Proc. Int. Joint Conf. Artif. Intell.*, 2018, pp. 396–402.
- [13] S. Chen, Y. Yu, D. Fridovich-Keil, and U. Topcu, "Soft-bellman equilibrium in affine markov games: Forward solutions and inverse learning," *arXiv preprint arXiv:2304.00163*, 2023.
- [14] T. Başar, "Affine incentive schemes for stochastic systems with dynamic information," *SIAM J. Control Optim.*, vol. 22, no. 2, pp. 199–210, 1984.
- [15] N. Nisan and A. Ronen, "Algorithmic mechanism design," *Games Econ. Behav.*, vol. 35, no. 1, pp. 359–379, 2015.
- [16] M. Lopes, F. Melo, and L. Montesano, "Active learning for reward estimation in inverse reinforcement learning," in *Proc. Eur. Conf. Mach. Learn. Knowl. Discovery Databases*. Springer Berlin Heidelberg, 2009, pp. 31–46.
- [17] R. Akrou, M. Schoenauer, and M. Sebag, "April: Active preference learning-based reinforcement learning," in *Proc. Eur. Conf. Mach. Learn. Knowl. Discovery Databases*. Springer, 2012, pp. 116–131.
- [18] D. Sadigh, A. Dragan, S. Sastry, and S. Seshia, "Active preference-based learning of reward functions," in *Robotics: Science and Systems XIII*, July 2017.
- [19] P. F. Christiano, J. Leike, T. Brown, M. Martic, S. Legg, and D. Amodei, "Deep reinforcement learning from human preferences," *Adv. Neural Inform. Process. Syst.*, vol. 30, 2017.
- [20] C. Daniel, M. Viering, J. Metz, O. Kroemer, and J. Peters, "Active reward learning," in *Robot.: Sci. Syst.*, vol. 98, 2014.
- [21] E. Bıyık and D. Sadigh, "Batch active preference-based learning of reward functions," in *Proc. Conf. Robot Learn.*. PMLR, 2018, pp. 519–528.
- [22] E. Bıyık, D. A. Lazar, D. Sadigh, and R. Pedarsani, "The green choice: Learning and influencing human decisions on shared roads," in *Proc. IEEE Conf. Decision Control*. IEEE, 2019, pp. 347–354.
- [23] M. Palan, G. Shevchuk, N. Charles Landolfi, and D. Sadigh, "Learning reward functions by integrating human demonstrations and preferences," in *Robot.: Sci. Syst.*, 2019.
- [24] S. M. Katz, A.-C. Le Bihan, and M. J. Kochenderfer, "Learning an urban air mobility encounter model from expert preferences," in *Proc. IEEE/AIAA Digit. Avionics Syst. Conf.*. IEEE, 2019, pp. 1–8.
- [25] C. Basu, E. Bıyık, Z. He, M. Singhal, and D. Sadigh, "Active learning of reward dynamics from hierarchical queries," in *Proc. IEEE/RSJ Int. Conf. Intell. Robots Syst.*. IEEE, 2019, pp. 120–127.
- [26] R. Cohn, E. Durfee, and S. Singh, "Comparing action-query strategies in semi-autonomous agents," in *Proc. AAAI Conf. on Artif. Intell.*, vol. 25, no. 1, 2011, pp. 1102–1107.
- [27] C. Daniel, O. Kroemer, M. Viering, J. Metz, and J. Peters, "Active reward learning with a novel acquisition function," *Autonomous Robots*, vol. 39, pp. 389–405, 2015.
- [28] Y. Cui and S. Niekum, "Active reward learning from critiques," in *Proc. IEEE Int. Conf. Robot. Automat.*. IEEE, 2018, pp. 6907–6914.
- [29] E. Bıyık, M. Palan, N. C. Landolfi, D. P. Losey, and D. Sadigh, "Asking easy questions: A user-friendly approach to active reward learning," in *Conf. Robot Learn.*. PMLR, 2020, pp. 1177–1190.
- [30] V. Myers, E. Bıyık, N. Anari, and D. Sadigh, "Learning multimodal rewards from rankings," in *Proc. Conf. Robot Learn.*. PMLR, 2022, pp. 342–352.
- [31] R. Horst and N. V. Thoai, "Dc programming: overview," *J. Optim. Theory Appl.*, vol. 103, pp. 1–43, 1999.
- [32] T. Lipp and S. Boyd, "Variations and extension of the convex–concave procedure," *Optim. Eng.*, vol. 17, pp. 263–287, 2016.
- [33] J. V. Neumann and O. Morgenstern, *Theory of Games and Economic Behavior*. Princeton University Press, 1944.
- [34] R. D. Luce, *Individual Choice Behavior: A Theoretical Analysis*. Wiley, 1959.
- [35] B. D. Ziebart, A. L. Maas, J. A. Bagnell, and A. Dey, "Maximum entropy inverse reinforcement learning," in *Proc. AAAI Conf. on Artif. Intell.*, vol. 3, 2008, pp. 1433–1438.
- [36] M. Wulfmeier, P. Ondruska, and I. Posner, "Maximum entropy deep inverse reinforcement learning," *arXiv preprint arXiv:1507.04888[cs.LG]*, 2015.
- [37] Z. Wu, L. Sun, W. Zhan, C. Yang, and M. Tomizuka, "Efficient sampling-based maximum entropy inverse reinforcement learning with application to autonomous driving," *IEEE Robot. Automat. Lett.*, vol. 5, no. 4, pp. 5355–5362, 2020.
- [38] S. Dempe and A. Zemkoho, "Bilevel optimization," in *Springer Optimization and Its Applications*. Springer, 2020, vol. 161.
- [39] G. Lanckriet and B. K. Sriperumbudur, "On the convergence of the concave-convex procedure," *Adv. Neural Inform. Process. Syst.*, vol. 22, 2009.
- [40] J. Bezanson, A. Edelman, S. Karpinski, and V. B. Shah, "Julia: A fresh approach to numerical computing," *SIAM review*, vol. 59, no. 1, pp. 65–98, 2017. [Online]. Available: <https://doi.org/10.1137/141000671>
- [41] M. Lubin, O. Dowson, J. Dias Garcia, J. Huchette, B. Legat, and J. P. Vielma, "JuMP 1.0: Recent improvements to a modeling language for mathematical optimization," *Math. Program. Comput.*, 2023.
- [42] M. ApS, *MOSEK Optimizer API for Julia 10.2.3*, 2024. [Online]. Available: <https://docs.mosek.com/latest/juliaapi/index.html>

- [43] Y. Pyo, D. Lim, T. Lim, and K. Gil, “turtlebot3_description,” http://wiki.ros.org/turtlebot3_description, 2024.
- [44] J. Levy, “Rossockets.jl,” <https://github.com/CLeARoboticsLab/RosSockets.jl>, 2024.
- [45] —, “ros_sockets,” https://github.com/CLeARoboticsLab/ros_sockets, 2024.
- [46] T. Fischer, W. Vollprecht, S. Traversaro, S. Yen, C. Herrero, and M. Milford, “A robostack tutorial: Using the robot operating system alongside the conda and jupyter data science ecosystems,” *IEEE Robot. Automat. Mag.*, 2021.
- [47] C. M. Bishop and N. M. Nasrabadi, *Pattern recognition and machine learning*. Springer, 2006, vol. 4, no. 4.